JOURNAL OF SCIENCE TECHNOLOGY AND EDUCATION 11(1), MARCH, 2023
ISSN: 2277-0011; Journal homepage: www.atbuftejoste.net

Development of a Rotor Flux- Oriented Control Method for Efficiency Improvement of a Three Phase Induction Motor

F.O. Balogun[1]*, G. A. Olarinoye[2], A. S. Abubakar[3]
Department of Electrical Engineering,
Faculty of Engineering,
Ahmadu Bello University, Zaria.

ABSTRACT
The efficiency of induction motor IM drives under variable operating load conditions can be improved by predicting the optimum flux that guarantees loss minimization, leading to maximizing the efficiency of three phase induction motors. This approach helps to achieve significant amount of savings in electric energy consumption. This research developed a method to optimize the flux of a three- phase induction motor and thereby maximize its efficiency for each load torque applied at a giving speed. Mathematical models for the conventional rotor flux-oriented control scheme, total power loss as a function of rotor flux and for optimum flux as a function of operating speed and load torque were analytically derived. A MATLAB/Simulink model of the proposed rotor flux optimization scheme was developed to verify the analyses set forth for a typical three-phase IM. The results of the proposed method were compared with those of the conventional rotor flux control method and direct torque control method in terms of loss reduction and efficiency for the same induction motor. The proposed rotor flux optimization scheme gave 8.51% improvement in efficiency compared to the conventional rotor flux control scheme at a speed of 250 rad/s for a load torque of 3Nm.It also gave 5.01% improvement in efficiency compared to the optimized DTC control scheme for the same speed and load torque. At a lower speed of 150 rad/s, power loss reduced by 17.1% while efficiency was higher by 5.7% for a load torque of 3Nm under the proposed scheme as compared to the optimized DTC scheme.

ARTICLE INFO
Article History
Received: September, 2022
Received in revised form: February, 2023
Accepted: March, 2023
Published online: March, 2023

KEYWORDS
Vector control, PI controller, Induction motor, Matlab, Simulink, DTC

INTRODUCTION

Induction motors are the most widely used electric machine in the industry, because of their ruggedness, less cost and very low maintenance cost. Studies have shown that bulks of energy consumed in the industry are consumed by induction motor and other electric machines (Engel, *et al.*, 2015,). Therefore, effort has been made over the years by various manufacturers of induction motors in the technique of construction of Energy Efficient Motors (EEM). This has resulted in improving efficiency, economic saving and profit. Induction motor have high efficiency at rated speed and torque, but the efficiency of induction motor decrease greatly at light loads because of an imbalance in copper and core loss. Energy saving can however, be achieved by proper selection of the flux level in the motor (Eseosa & Christian, 2018). Losses in induction motor are classified into: stator copper loss, rotor copper loss,

Corresponding author: Balogun, F. O.
Odunayobalogun2001@yahoo.com
Department of Electrical Engineering, Faculty of Engineering, Ahmadu Bello University, Zaria.
© 2023. Faculty of Tech. Education, ATBU Bauchi. All rights reserved

core loss, stray loss, and friction and windage loss. The copper and core losses account for the largest amount of losses in induction motor; hence interest in the analysis in this work. In order to increase and maintain the motor efficiency, the flux must be reduced, and balance obtain between copper loss and core losses. Basically, there are two approaches to improving the efficiency of induction motor. (Faduyile 2009,)

i) Loss based model approach or Loss model controller (LMC)
ii) Power measure-based approach or Search controller (SC)

In loss based model approach, the model base controller compute losses by using the machine model and selects a flux level that minimizes the losses LMC is fast and does not produce torque ripple, while for the power measure based approach, the controller searches for the operating points where the output power is constant (Rashtchi & Bizhani , 2015)

In this research, Loss based model approach or Loss model controller (LMC) of induction motor drive system, based on determining the optimal flux for loss minimization is applied.

Induction motors are the most widely used among all other types of motors in the world, and are often termed "the workhorse of industry". It is also used in transportation; household appliances and laboratories etc. Studies have shown that about 70% of electricity in industries is consumed by IM motor (Engel, *et al.*, 2015), therefore, a large amount of power is required to run them. The significance of this research is the reduction in energy consumed by the induction motor for the same applied load over the period of motor operation. This should go a long way to reduce operating cost and to make spare energy available to meet other energy demands. In the long term, this benefit should also slow the world overall energy growth/ consumption and protect the environment from pollution and preserve the world natural resources from further depletion.

Induction motors are large consumers of the electric energy, and are designed to operate efficiently at rated loads. Unfortunately, these motors operate on partial or low loads most of the time, this situation leads to inefficient motor operation with attendant losses in energy and increased operating cost. This research seeks to reduce the inefficiency of IM motor operation under the conditions of partial or low load operation by developing a method to optimize the efficiency of the motor under these conditions.

Several paper has been published in the related field, to mention but few among others. Rashtchi & Bizhani, (2015) presented a new online Loss Minimization Algorithm using Particle Swam Optimization (PSO) to determine the optimum flux level for the efficiency optimization of vector-controlled induction motor. Khan *et al.*, (2015) developed a high performance and robust control structure called the Flux Optimized Direct Torque Control (DTC) for induction motor. Lee, *et al.*, (2013) presented a Loss Base Model Controller (LMC) using Digital Signal Processor (DSP) TM320LF2812, for Induction motor efficiency maximization and energy saving. Sruthi *et al.*, (2017) formulated a Loss Minimization Algorithm for energy saving and efficiency improvement in induction motor drive. The input voltage and frequency are optimized to reduce total losses. (Eseosa &

Corresponding author: Balogun, F. O.
Odunayobalogun2001@yahoo.com
Department of Electrical Engineering, Faculty of Engineering, Ahmadu Bello University, Zaria.
© 2023. Faculty of Tech. Education, ATBU Bauchi. All rights reserved

JOURNAL OF SCIENCE TECHNOLOGY AND EDUCATION 11(1), MARCH, 2023
ISSN: 2277-0011; Journal homepage: www.atbuftejoste.net

Christian, (2018), Afify et al., 2018, Yadav, 2016 Nam & Uddin, 2006 and Laroui, et al., 2021) presented various approach in optimization control techniques to improve the efficiency operation of induction motor. Aygun & Aktas, (2018) implemented Direct Torque Control (DTC) combined with online Loss Minimization Model Based Controller (LMC) to minimize the losses of Electric Vehicle (EV) induction motors.

PROPOSED METHODS

Mathematical Model of Three Phase Induction Motor

The dynamics model of the induction motor in *d-q* coordinates established in a rotor flux-oriented reference frame is given by (Kalhoodashti & Shahbazian., 2011).

$$V_{qs} = R_s i_{qs} + \omega_e \lambda_{ds} + p\lambda_{qs} \quad (1)$$

$$V_{ds} = R_s i_{ds} - \omega_e \lambda_{qs} + p\lambda_{ds} \quad (2)$$

$$V'_{qr} = R'_r i'_{qr} + (\omega_e - \omega_r)\lambda'_{dr} + p\lambda'_{qr} \quad (3)$$

$$V'_{dr} = R'_r i'_{dr} - (\omega_e - \omega_r)\lambda'_{qr} + p\lambda'_{dr} \quad (4)$$

$$\lambda_{qs} = (L_{ms} + L_{ls})i_{qs} + L_{ms} i'_{qr} \quad (5)$$

$$\lambda_{ds} = (L_{ms} + L_{ls})i_{ds} + L_{ms} i'_{dr} \quad (6)$$

$$\lambda'_{qr} = L_{ms} i_{qs} + (L_{ms} + L'_{lr})i'_{qr} \quad (7)$$

$$\lambda'_{dr} = L_{ms} i_{ds} + (L_{ms} + L'_{lr})i'_{dr} \quad (8)$$

$$T_e = \frac{p}{2}\frac{L_{ms}}{L'_r}\left(\lambda'_{dr} i_{qs} - \lambda'_{qr} i_{qs}\right) \quad (9)$$

$$T_e = \frac{2j}{p} P\omega_r + T_L \quad (10)$$

Where V_{ds} and V_{qs}, V_{dr} and V_{qr} are the direct axes and quadrature axes stator and rotor voltages, and i_{ds} and i_{qs}, i_{dr} and i_{qr} are stator and rotor currents, λ_{ds} and λ_{qs}, λ_{dr} and λ_{qr} are stator and rotor flux respectively, R_s , R_r are stator and rotor resistance, ω_e is stator frequency ω_r is the rotor electrical speed

The equivalent circuit obtained from the mathematical model equations (1) - (8) of the IM is shown in Figure 1

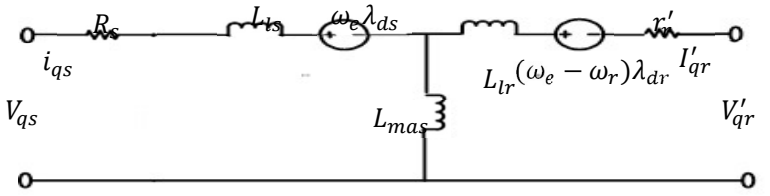

(b) d - axis equivalent circuit

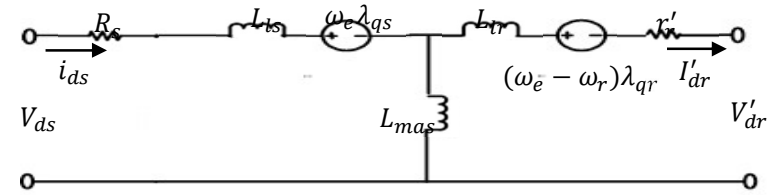

Figure 1: Equivalent circuit of induction motor in d-q frame.

Corresponding author: Balogun, F. O.
Odunayobalogun2001@yahoo.com
Department of Electrical Engineering, Faculty of Engineering, Ahmadu Bello University, Zaria.
© 2023. Faculty of Tech. Education, ATBU Bauchi. All rights reserved

Development of a rotor flux-oriented control scheme for the three-phase induction motor

The development of the rotor flux-oriented control scheme for the three-phase induction motor presented in this subsection. The scheme is derived from the rotor dynamic equations of the three-phase induction machine in the synchronously rotating reference frame represented by equations (3-4 and 7-8) which are re-written below for convenience.

$$V_{qr}'^{e} = R'_r i_{qr}'^{e} + (\omega_e - \omega_r)\lambda_{dr}'^{e} + p\lambda_{qr}'^{e} \quad (11)$$

$$V_{dr}'^{e} = R'_r i_{dr}'^{e} - (\omega_e - \omega_r)\lambda_{qr}'^{e} + p\lambda_{dr}'^{e} \quad (12)$$

$$\lambda_{qr}'^{e} = L_r i_{qr}'^{e} + L_m i_{qs}^{e} \quad (13)$$

$$\lambda_{dr}'^{e} = L_r i_{dr}'^{e} + L_m i_{ds}^{e} \quad (14)$$

The q-axis component of the rotor flux space vector $\lambda_{qr}'^{e}$ is equated zero because of the alignment of the d-axis with the rotor flux vector. It is mathematically represented as follows;

$$\lambda_{qr}'^{e} = 0 \quad (15)$$

Figure 2 shows the rotor flux and stator current space vectors in the synchronous reference frame when the d-axis is aligned with the rotor flux vector.

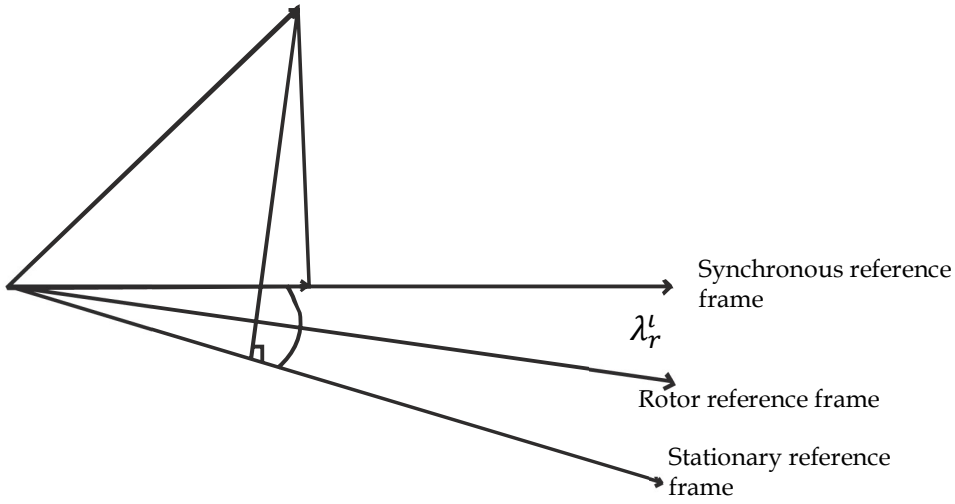

Figure 2: d-axis alignment with the rotor flux vector

The d-axis component of the rotor flux space vector $\lambda_{dr}'^{e}$ is now equal to the rotor flux magnitude $\lambda_r'^{e}$. The rotor flux magnitude is expressed as follows;

$$\lambda_r'^{e} = \sqrt{\lambda_{qr}'^{e^2} + \lambda_{dr}'^{e^2}} \quad (16)$$

Mathematically, applying equation (15) to equations (11-13and 16) yield the following results;

$$\lambda_r'^{e} = \lambda_{dr}'^{e}. \quad (17)$$

$$0 = R'_r l_{qr}'^{e} + (w_e - w_r)\lambda_r^{e\prime} \quad (18)$$

$$0 = R'_r l_{dr}'^{e} + \rho\lambda_{dr}^{e\prime} \quad (19)$$

$$\lambda_r^{e\prime} = L_m l'_{ds} + L_r l_{dr}^{e} \quad (20)$$

Corresponding author: Balogun, F. O.
Odunayobalogun2001@yahoo.com
Department of Electrical Engineering, Faculty of Engineering, Ahmadu Bello University, Zaria.
© 2023. Faculty of Tech. Education, ATBU Bauchi. All rights reserved

JOURNAL OF SCIENCE TECHNOLOGY AND EDUCATION 11(1), MARCH, 2023
ISSN: 2277-0011; Journal homepage: www.atbuftejoste.net

$$0 = L_m l_{qs}^e + L_r l_{qr}' \quad (21)$$

Equations (18-19) have been obtained considering that the short-circuited squirrel cage rotor of the three-phase induction motor have zero voltages in the q and d axis of the rotor windings i.e. $V_{qr}^{e\prime} = 0$ and $V_{dr}^{e\prime} = 0$.

The rotor flux dynamics is developed from equations (19) and (20) to give the following;

$$\frac{\tau_r d\lambda_r^{e\prime}}{dt} + \lambda_r^{e\prime} = L_m l_{ds} \quad (22)$$

where $\tau_r = \frac{L_r}{R_r}$ (23)

The dynamics are those of first order system governed by rotor time constant τ_r. The Slip frequency ω_s is obtained from equations (18) and (21) as follows;

$$w_s = w_e - w_r = \frac{R_r' L_m l_{qs}^e}{L_r' \lambda_r^{e\prime}} \quad (24)$$

The rotor flux angle θ_e, which is also the angle of transformation because of alignment of the d-axis to the rotor flux vector, is estimated by integrating the rotor flux angular frequency as follows

$$\theta_e = \int \omega_e \, dt = \int \left(\omega_r + \frac{R_r' L_m l_{qs}^e}{L_r' \lambda_r^{e\prime}}\right) dt \quad (25)$$

The torque produced in the three-phase induction motor given by equation (2.18) is modified, upon application of equations (15) and (17), to the following;

$$T_{em} = \frac{3P}{4} \frac{L_m}{L_r} \lambda_r'^e i_{qs}'^e \quad (26)$$

As a result of the alignment of the rotor flux magnitude with the d-axis, equations (23-25) enables the estimation of rotor flux magnitude and the phase angle or the angle of transformation. The estimation of the rotor flux magnitude and phase angle is illustrated in Figure 3.

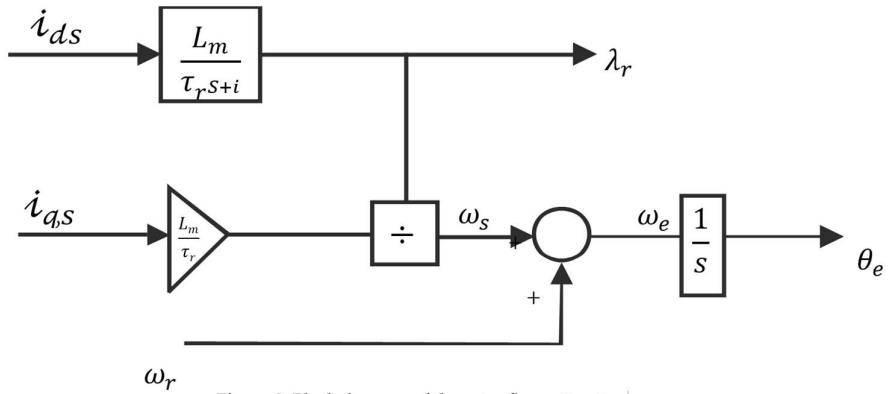

Figure 3: Block diagram of the rotor flux estimation

Activate Windows

Development of a rotor flux optimization scheme

The objective of the flux optimization scheme is to regulate the flux magnitude such that minimum losses occur for a given torque. The three-phase induction motor equivalent circuit was re-drawn to

Corresponding author: Balogun, F. O.
Odunayobalogun2001@yahoo.com
Department of Electrical Engineering, Faculty of Engineering, Ahmadu Bello University, Zaria.
© 2023. Faculty of Tech. Education, ATBU Bauchi. All rights reserved

JOURNAL OF SCIENCE TECHNOLOGY AND EDUCATION 11(1), MARCH, 2023
ISSN: 2277-0011; Journal homepage: www.atbuftejoste.net

account for the core loss resistancer_c. The equivalent circuit with core loss resistance is presented in figure 1. As a result, the voltage, flux linkage and torque equations of the motor are reformulated to account for the effect of the core loss resistance.

The following voltage, flux linkage and current equations are obtained from the equivalent circuits of figures 1 (a) and (b) and equations (1-4) give the following equations

a) Voltage Equations

$$V_{qs}^{e} = r_s i_{qs}^{e\prime} + \mathrm{k}\omega_e \lambda_{ds}^{e} + kp\lambda_{qs}^{e} \quad (27)$$

$$V_{ds}^{e} = r_s i_{ds}^{e\prime} - \mathrm{k}\omega_e \lambda_{qs}^{e} + kp\lambda_{ds}^{e} \quad (28)$$

$$0 = r_r{}' i_{qr}^{e\prime} + (\omega_e - \omega_r)\lambda_{dr}^{e\prime} + p\lambda_{qr}^{e\prime} \quad (29)$$

$$0 = r_r{}' i_{dr}^{e\prime} - (\omega_e - \omega_r)\lambda_{qr}^{e\prime} + p\lambda_{dr}^{e\prime} \quad (30)$$

b) Current Equations

The currents i_{cq} and i_{cd} flowing through the core loss branches are obtained from the equivalent circuits and are given as follows;

$$i_{cq} = i_{qs}^{e} - i_{qs}^{e\prime} \quad (31)$$

$$i_{cd} = i_{ds}^{e} - i_{ds}^{e\prime} \quad (32)$$

$$i_{cq} = \frac{V_{qs}^{e}}{kr_c} \quad (33)$$

$$i_{cd} = \frac{V_{ds}^{e}}{kr_c} \quad (34)$$

$$\text{Where } k = 1 + \frac{r_s}{r_c} \quad (35)$$

Currents $i_{qs}^{e\prime}$ and $i_{ds}^{e\prime}$ are the torque currents responsible for producing electromagnetic torque in the motor as seen from the equivalent circuit of figure 1 (a) and (b).

For the purpose of analysis, an ideal inverter has been assumed. The difficulties associated with the modelling and implementation of the practical inverter has been carefully avoided in this work. The ideal inverter supplies the controlled three phase voltages to the three-phase induction motor in such a way that the flux is regulated at its optimum value for each load torque. The torque command is the output of the speed control loop. When the motor drive is in operation, flux is produced in the machine. The flux is controlled to its optimum value by regulating the d-axis stator current. This regulation ensures linear control of torque by the q-axis stator current. The flux model receives stator currents i_{qs}^{e}, i_{ds}^{e} and speed ω_r and delivers the flux $\lambda_r^{\prime e*}$, supply frequency ω_e and the corresponding angular position θ_e, to ensure proper vector alignment and transformation of stationary reference frame variables to synchronously rotating reference frame variables thereby keeping the integrity of the control scheme. θ_e is used in the transformation block while ω_e is utilized in the decoupling block to decouple the dynamics of i_{qs}^{e} and i_{ds}^{e}. The Simulink implementation of the proposed drive scheme is shown in Figure 4.

Corresponding author: Balogun, F. O.
Odunayobalogun2001@yahoo.com
Department of Electrical Engineering, Faculty of Engineering, Ahmadu Bello University, Zaria.
© 2023. Faculty of Tech. Education, ATBU Bauchi. All rights reserved

JOURNAL OF SCIENCE TECHNOLOGY AND EDUCATION 11(1), MARCH, 2023
ISSN: 2277-0011; Journal homepage: www.atbuftejoste.net

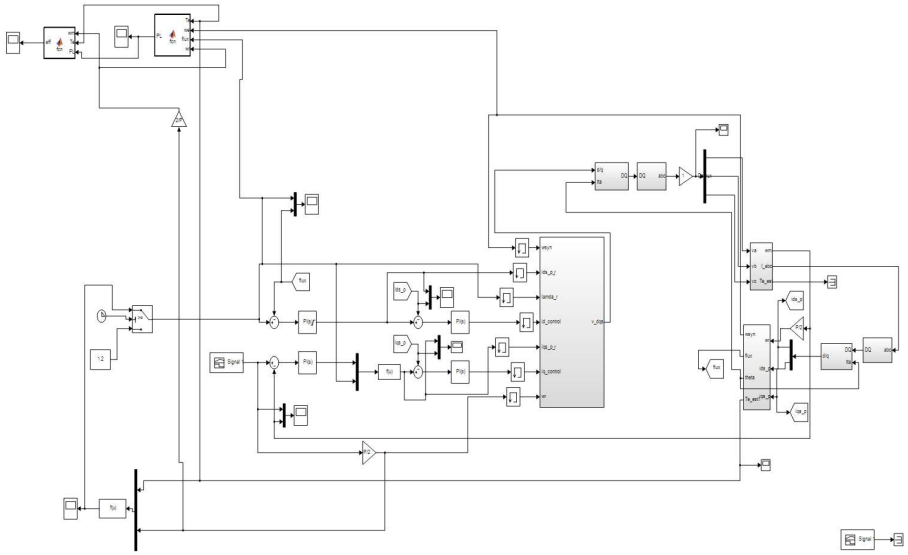

Figure 4: Simulink implementation of the proposed drive scheme

Figure 4 was programmed in MATLAB/Simulink environment. It consists of the three-phase motor model, flux estimation model, optimal flux calculation function block, decoupling block and the transformation block. These models were programmed as well and are provided in Figures 5– 9 respectively.

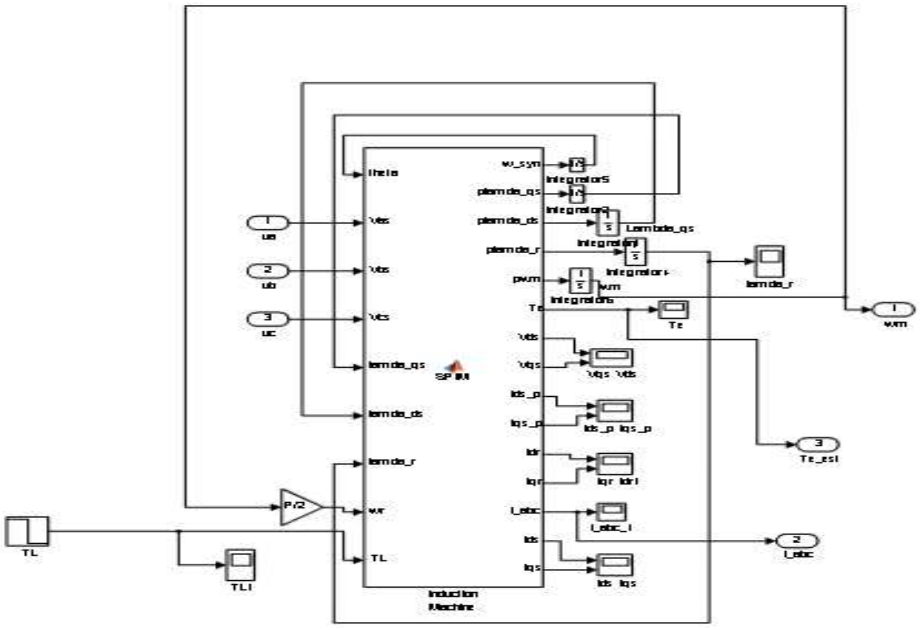

Figure 5: Three phase induction motor model

Corresponding author: Balogun, F. O.
Odunayobalogun2001@yahoo.com
Department of Electrical Engineering, Faculty of Engineering, Ahmadu Bello University, Zaria.
© 2023. Faculty of Tech. Education, ATBU Bauchi. All rights reserved

JOURNAL OF SCIENCE TECHNOLOGY AND EDUCATION 11(1), MARCH, 2023
ISSN: 2277-0011; Journal homepage: www.atbuftejoste.net

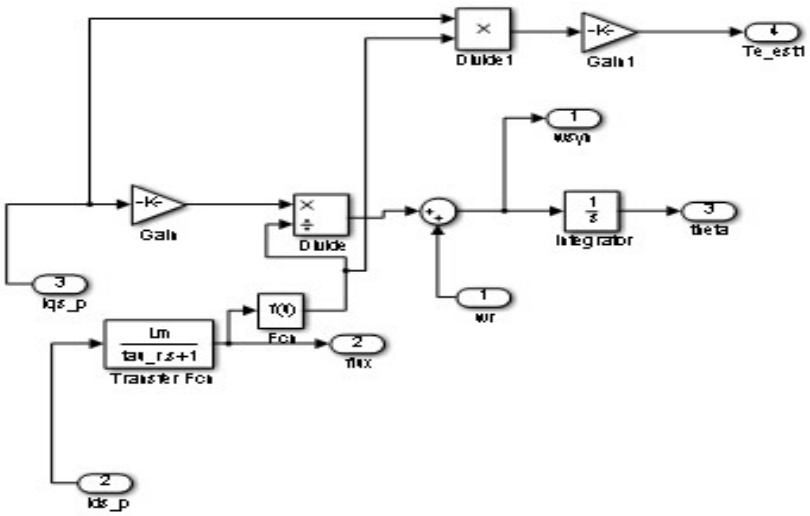

Figure 6: Flux estimation model

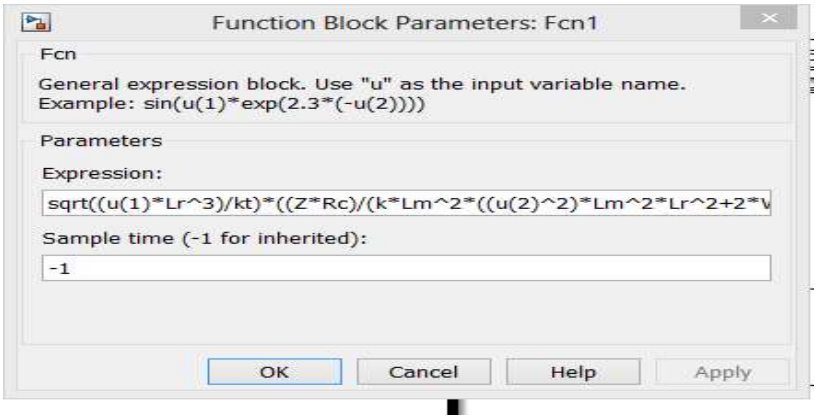

Figure 7: Optimal flux calculation function block

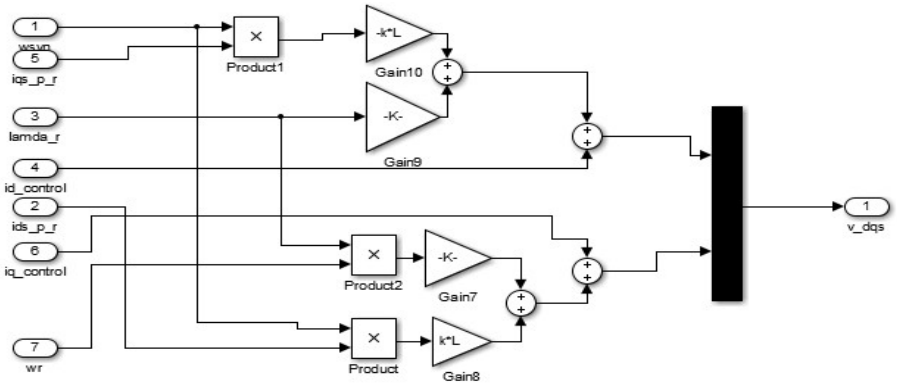

Figure 9: Decoupling block

Corresponding author: Balogun, F. O.
Odunayobalogun2001@yahoo.com
Department of Electrical Engineering, Faculty of Engineering, Ahmadu Bello University, Zaria.
© 2023. Faculty of Tech. Education, ATBU Bauchi. All rights reserved

JOURNAL OF SCIENCE TECHNOLOGY AND EDUCATION 11(1), MARCH, 2023
ISSN: 2277-0011; Journal homepage: www.atbuftejoste.net

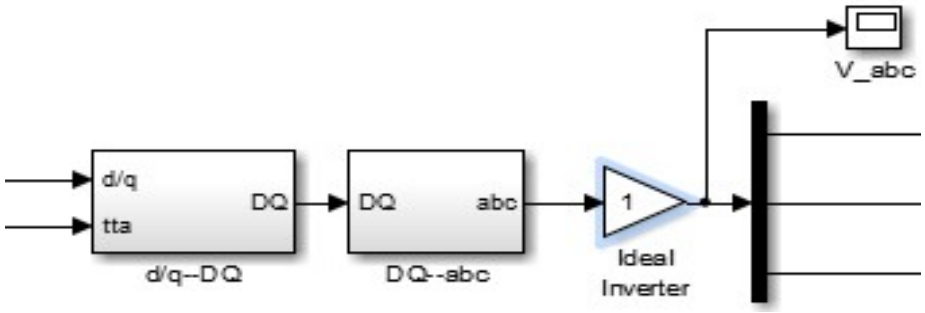

Figure 9: Transformation block

RESULTS AND DISCUSSION

In this section, the effectiveness of the proposed method is discussed, and relevant results reported. Simulation results are presented and discussed.

Simulation Results

The motor parameters utilized in order to verify the effectiveness of the proposed scheme are provided in Table 1.

Table 1: Induction Motor Parameters.

S/N	Parameters		S/N	Parameters	
1	Voltage	400V	7	r_r	1.52Ω
2	Frequency	50HZ	8	r_c	13400Ω
3	Synchronous speed	3000rpm	9	$L_s = L_r$	0.2405H
4	No of poles	2	10	L_m	0.2323H
5	Power	3kW	11	J	0.0044kgm^2
6	r_s	1.795Ω	12		

Controller Design

The controller gains determined from the derived equations and are tabulated in Table 2

Table 2: Current, speed and flux controller gains

Controller	Proportional gain	Integral gain
q-axis current controller (k_I, k_p)	639.4058	6.3958e+06
d-axis current controller (k_I, k_p)	639.4058	6.3958e+06
Speed controller (k_I, k_p)	1.76	176
Flux controller (k_I, k_p)	268.1424	2.7245e+04

The unit step response of the current, speed and flux control systems are plotted in Figures 10-12. It can be seen that the step response tracks its reference for each controller. Associated system performance indices were calculated using the control system tool box in MATLAB and are provided in Tables 3-5 for the current, flux and speed control systems respectively.

Corresponding author: Balogun, F. O.
Odunayobalogun2001@yahoo.com
Department of Electrical Engineering, Faculty of Engineering, Ahmadu Bello University, Zaria.
© 2023. Faculty of Tech. Education, ATBU Bauchi. All rights reserved

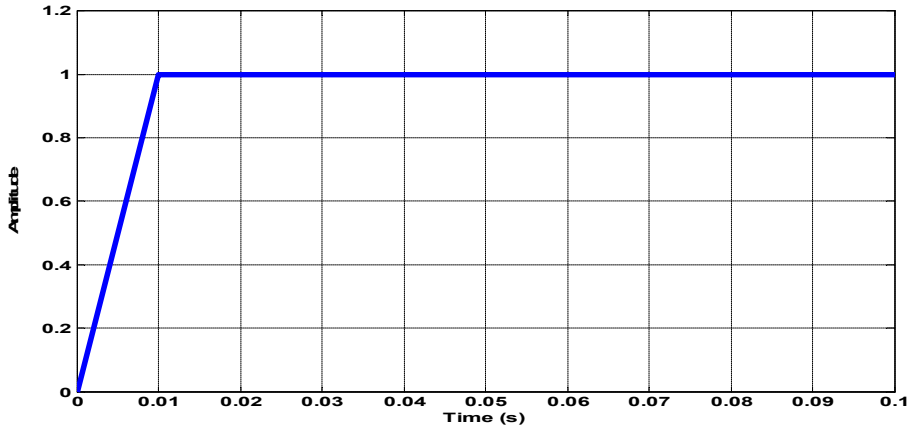

Figure 10: Unit step response of the current control loop

Table 3: Command-tracking performance of the current control loop

Performance Index	Value
Rise Time	0.008s
Maximum Overshoot	0
Peak Time	0.01s
Settling Time	0.01s
Steady State Error	1.1102e-14

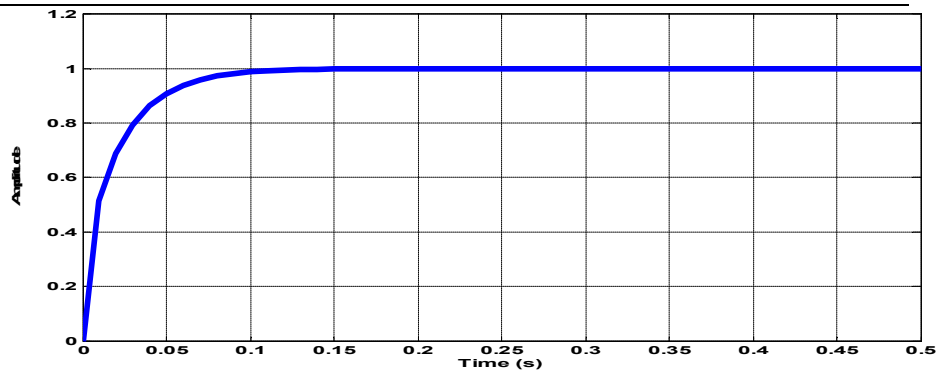

Figure 4.2: Unit step response of the speed control loop

Table 4: Command-tracking performance of the speed control loop

Performance Index	Value
Rise Time	0.0461s
Maximum Overshoot	0
Peak Time	0.5s
Settling Time	0.09s
Steady State Error	9.9359e-08

The unit step response of the speed control loop is seen to reach steady state slower than that of the current control loop.

Corresponding author: Balogun, F. O.
Odunayobalogun2001@yahoo.com
Department of Electrical Engineering, Faculty of Engineering, Ahmadu Bello University, Zaria.
© 2023. Faculty of Tech. Education, ATBU Bauchi. All rights reserved

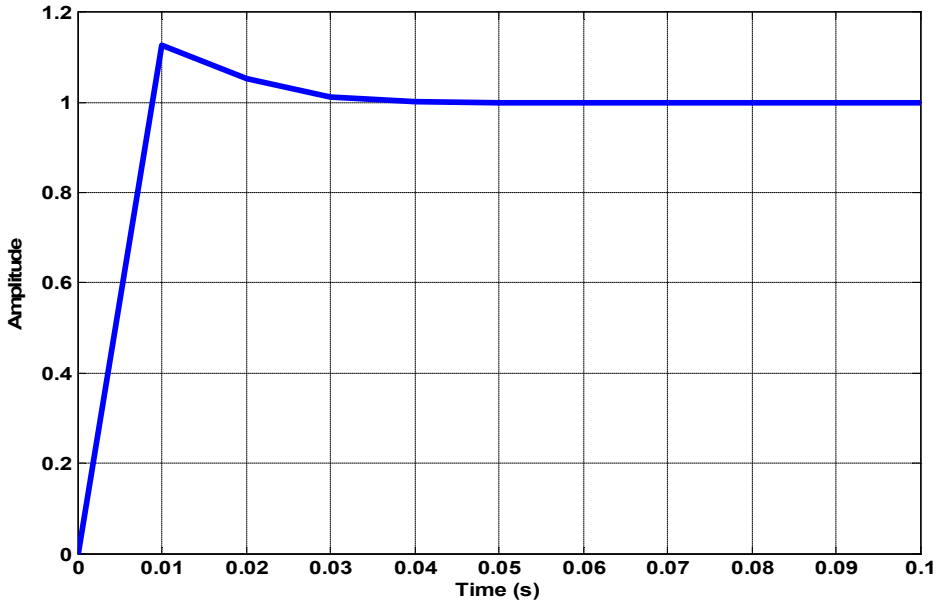

Figure 12: Unit step response of the flux control loop

Table 5: Command-tracking performance of the flux control loop

Performance Index	Value
Rise Time	0.0071s
Maximum Overshoot	12.6782%
Peak Time	0.01s
Settling Time	0.03s
Steady State Error	3.7859e-06%

The step response of the flux control loop is observed to exhibit an overshoot of 12.6782%. It reaches steady state slower than the step response of the current control loop as well.

Rotor flux optimization scheme performance results

The reference speed was set to 250 rad/s and the load torque was set to 3Nm. The loss minimization function was set to trigger at 2.5s. The flux under rated conditions was calculated from Equation (2.20) as 1Wb. For a load torque of 3Nm, the result of power loss is provided in Figure 13

Corresponding author: Balogun, F. O.
Odunayobalogun2001@yahoo.com
Department of Electrical Engineering, Faculty of Engineering, Ahmadu Bello University, Zaria.
© 2023. Faculty of Tech. Education, ATBU Bauchi. All rights reserved

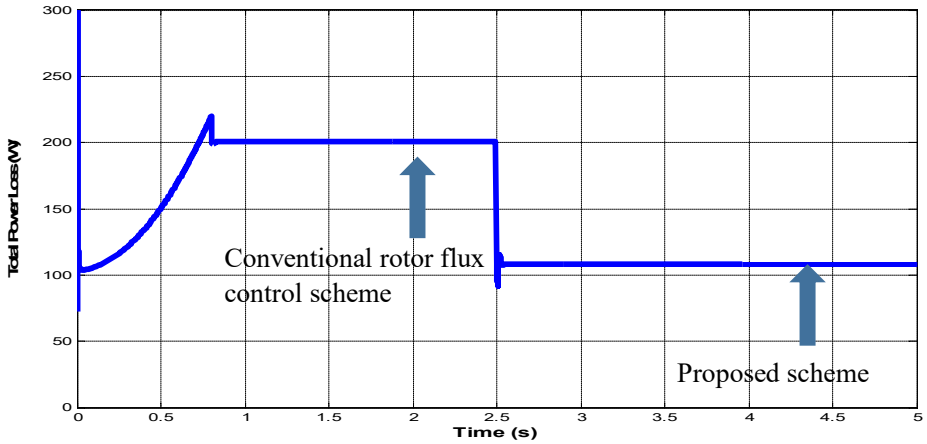

Figure 13: Electrical power loss in the induction motor with time

It can be seen that the conventional rotor flux control scheme produces a steady state power loss of 200W in the motor. The proposed scheme on the other hand, upon activation at a time of 2.5s produces a power loss of 108.04W in the same motor. This gives a significant reduction of 54.02%, and as a result, motor efficiency rises from 78.9% to 87.41% as shown in Figure 14

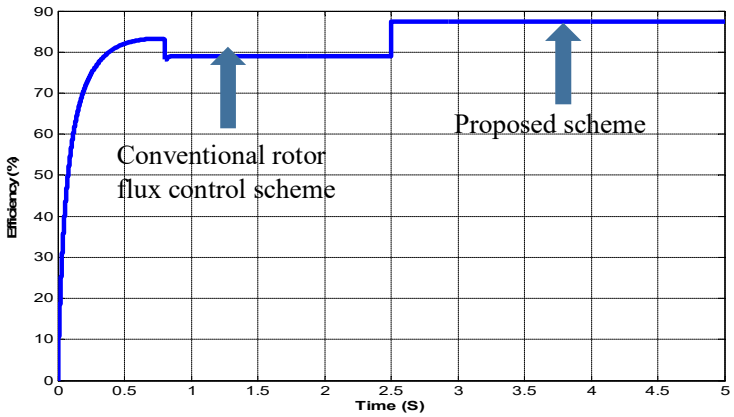

Figure 14: Efficiency of induction motor with time

Figure 15 shows the plot of the rotor flux. It can be seen that the flux value is 1Wb until the proposed scheme is activated and the flux reduces significantly to its optimal value of 0.6357Wb for the given load torque. This verifies the analysis set forth in chapter three that there is an optimal flux in the motor for which electrical losses are minimized and hence efficiency is maximized for a given load torque.

Corresponding author: Balogun, F. O.
Odunayobalogun2001@yahoo.com
Department of Electrical Engineering, Faculty of Engineering, Ahmadu Bello University, Zaria.
© 2023. Faculty of Tech. Education, ATBU Bauchi. All rights reserved

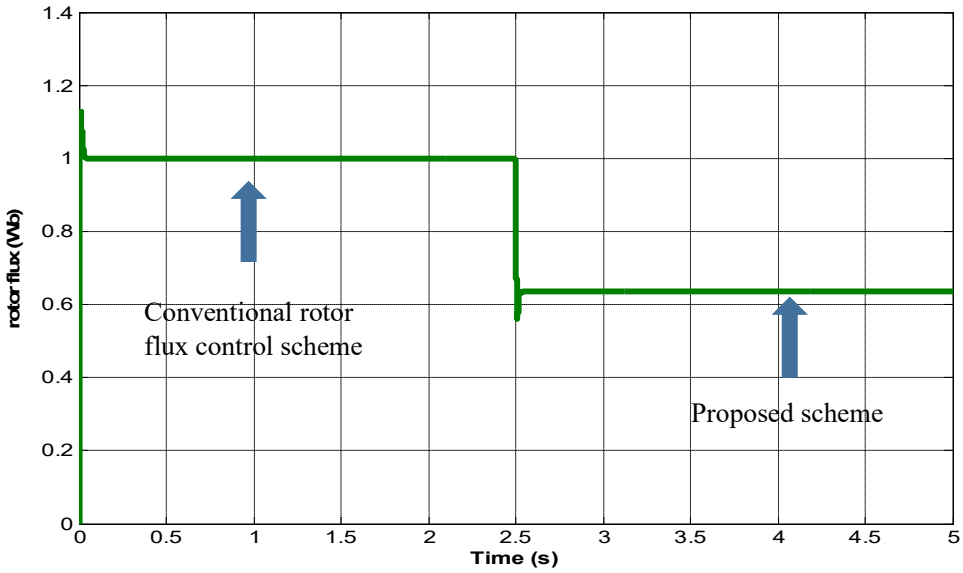

Figure 15: Rotor flux in the induction motor

Figure 16 shows the speed profile of the induction motor and it can be seen that the motor was set to accelerate and reach steady state speed of 250 rad/s at 0.8s.

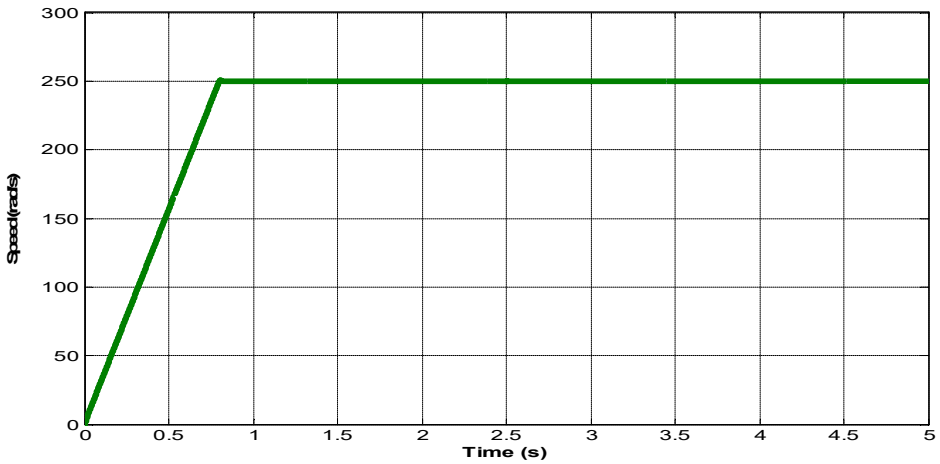

Figure 16: Speed Profile of induction motor

Figure 17 shows the torque produced in the motor during the simulation time. The steady state torque can be seen to equal 3Nm. A transient occurs during the time of activation of the proposed scheme at 2.5s of simulation time.

Corresponding author: Balogun, F. O.
Odunayobalogun2001@yahoo.com
Department of Electrical Engineering, Faculty of Engineering, Ahmadu Bello University, Zaria.
© 2023. Faculty of Tech. Education, ATBU Bauchi. All rights reserved

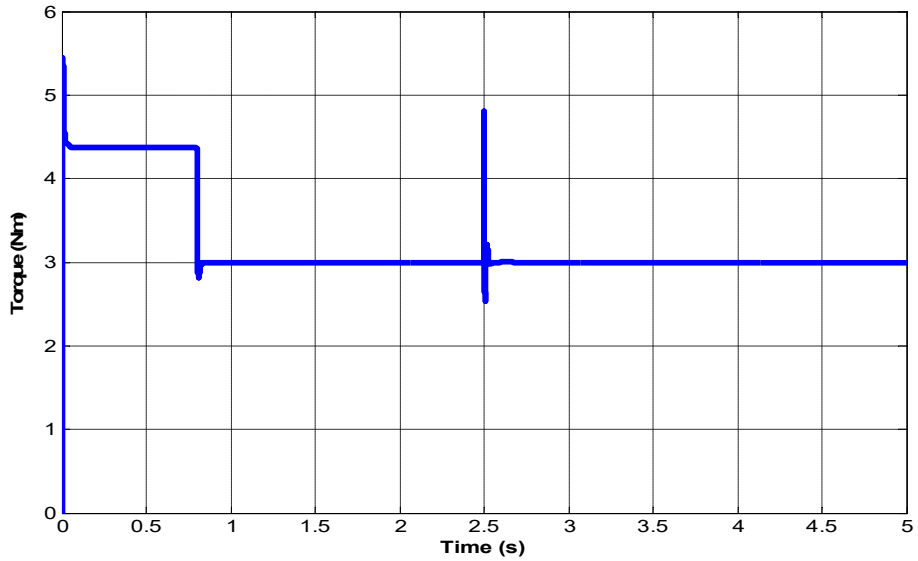

Figure 17: Torque produced in the motor with time

Table 6: Comparison of result between conventional and proposed rotor flux control scheme and the conventional and optimized DTC control schemes

Variable	Conventional rotor flux control scheme	Proposed method (Rotor flux-oriented control method)	Conventional DTC	Aygun's & Aktas method (Optimized DTC)
Total Power loss (W)	200	108.04	231.1961	166.2806
Efficiency (%)	78.9	87.41	77.1	82.4
Flux (Wb)	1	0.6357	1	0.7539

Table 6 shows a comparison of results between conventional and proposed rotor flux-oriented control scheme and the conventional and optimized DTC control schemes for the same motor parameters, reference speed and load torque. It can be observed that the proposed method gives a superior motor performance. The proposed rotor flux optimization scheme gives 8.51% improvement in efficiency compared to the conventional rotor flux control scheme at a speed of 250rad/s, for a load torque of 3Nm. The proposed scheme also gives a 5.01% improvement in efficiency compare to the optimized DTC control scheme proposed in Aygun and Aktas (2018).

The Performance of the Proposed Scheme at Variable Speed

Figures 18-21 show the performances of the motor under the proposed scheme at variable speeds. The rotor flux-oriented control scheme enables the variation of motor speed. To this end, the motor speed was ramped down from 250 rad/s to 150 rad/s and allowed to stay at that speed

Corresponding author: Balogun, F. O.
Odunayobalogun2001@yahoo.com
Department of Electrical Engineering, Faculty of Engineering, Ahmadu Bello University, Zaria.
© 2023. Faculty of Tech. Education, ATBU Bauchi. All rights reserved

between 4 and 5s of simulation time as seen in the Figure 18.

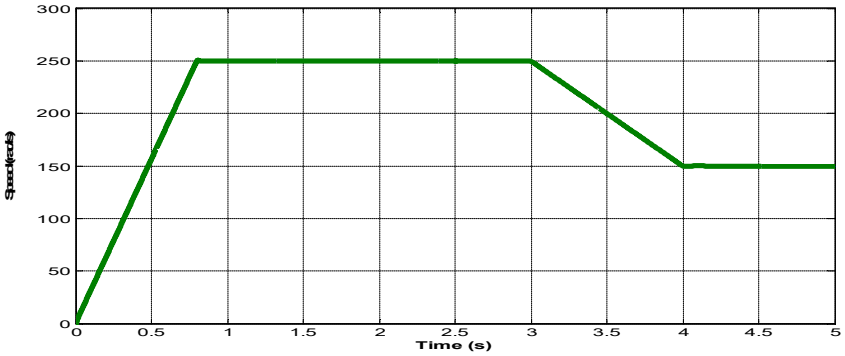

Figure 18: Variable speed profile of the induction motor

The total power loss is plotted in Figure 19 and it can be seen to reduce from 200W to 108.04W as in the previous result but it further reduces to 83.645W because of the drop in speed. The total power loss therefore reduces by 22.6% and this implies that there is an opportunity to save power when the motor is driven at a lower speed.

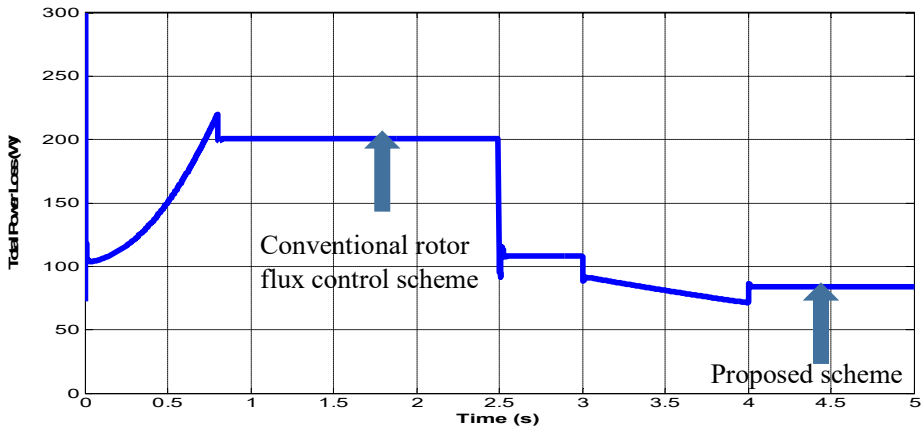

Figure 4.10: Total electric power loss under under variable speed.

The efficiency of the motor is plotted in Figure 20. It can be seen to decrease to a value of 84.8% after the motor speed is dropped to 150 rad/s because the power output drops with speed. A table of comparison between these results and those obtained in Aygun and Aktas (2018) is provided in Table 7.

Corresponding author: Balogun, F. O.
Odunayobalogun2001@yahoo.com
Department of Electrical Engineering, Faculty of Engineering, Ahmadu Bello University, Zaria.
© 2023. Faculty of Tech. Education, ATBU Bauchi. All rights reserved

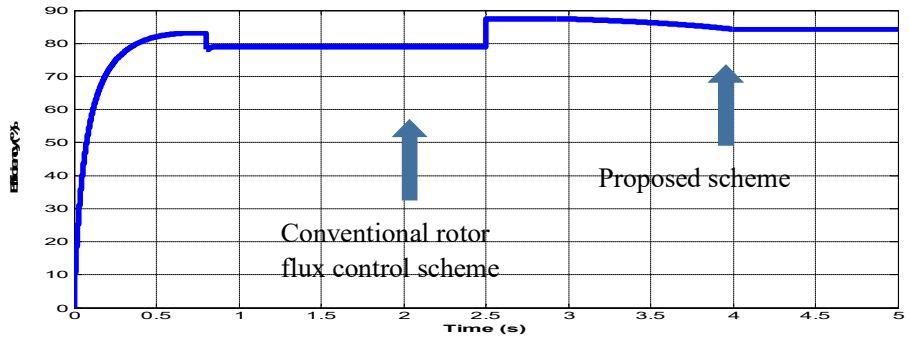

Figure 20: Efficiency of induction motor under variable speed

Table 7: Comparison of results of the proposed rotor flux-oriented control scheme with those of the optimized DTC at variable speed

Scheme	Total power loss (W)	Efficiency (%)
Proposed scheme at 250 rad/s	108.04	87.41
Proposed scheme at 150 rad/s	83.645	84.8
Optimized DTC at 250 rad/s	166.28	82.4
Optimized DTC at 150 rad/s	101	79.1

Table 7 shows the superior performance of the proposed method at variable speed when compared with the performance of the optimized DTC method under the same operating conditions. At a lower speed of 150 rad/s, power loss reduces by 17.2% while efficiency is higher by 5.7% for a load torque of 3Nm under the proposed scheme as compared to the optimized DTC scheme developed in Aygun and Aktas (2018).

The Performance of the Proposed Method at Variable Load

Figures 21-24 show the effectiveness of the proposed optimization scheme at varying loads. The load torque on the motor is reduced from 3Nm to 2Nm as shown in Figure 21.

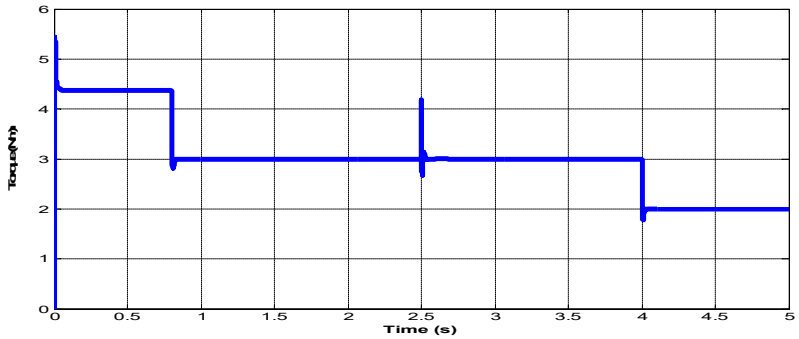

Figure 21: Torque Produced in the motor with load torque varying from 3Nm to 2Nm

In Figure 22, the total power loss is observed to decrease to 72.03 W after the initiation of the loss minimization function because the flux in the motor is optimized for each load torque. The optimal flux for the 2Nm

Corresponding author: Balogun, F. O.
Odunayobalogun2001@yahoo.com
Department of Electrical Engineering, Faculty of Engineering, Ahmadu Bello University, Zaria.
© 2023. Faculty of Tech. Education, ATBU Bauchi. All rights reserved

load is 0.5188 Wb as seen in Figure 24. The total loss reduces after the reduction in load from 3Nm to 2Nm because of the reduced output power.

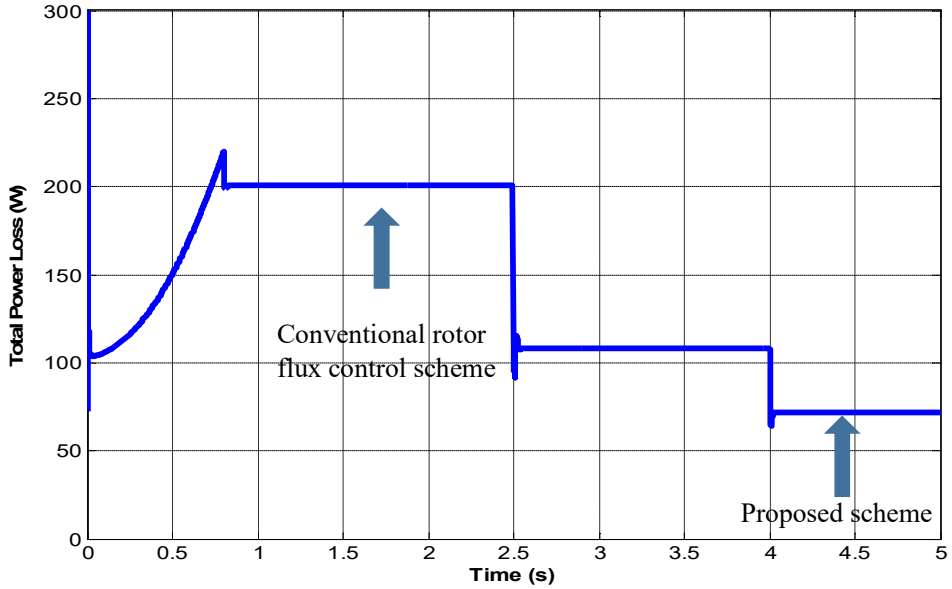

Figure 22: Total power loss with load torques varying from 3Nm to 2Nm

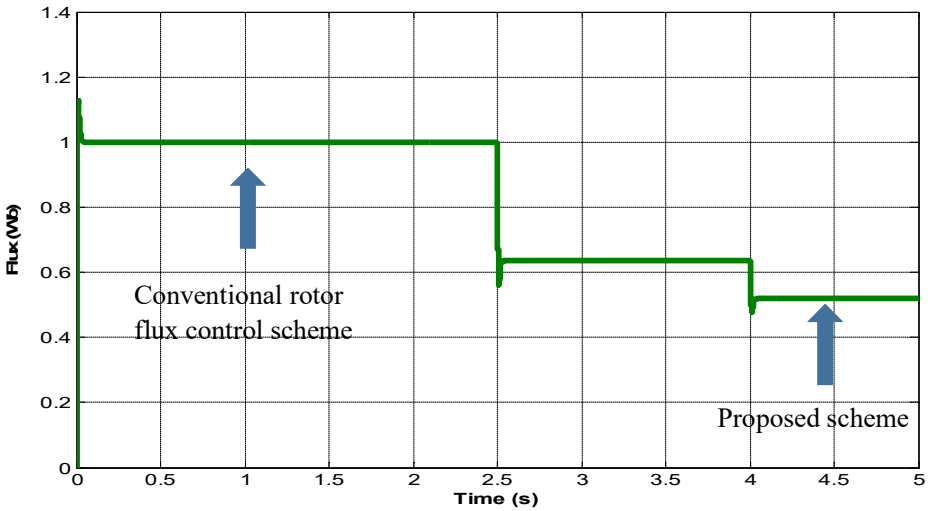

Figure 24: Optimal flux of induction motor with load torque varying from 3Nm to 2Nm

Although the motor operates at a lower load torque, the operating efficiency is observed to be the same as that for the 3Nm load torque. The value is still 87.41% as seen from Figure 25.

Corresponding author: Balogun, F. O.
Odunayobalogun2001@yahoo.com
Department of Electrical Engineering, Faculty of Engineering, Ahmadu Bello University, Zaria.
© 2023. Faculty of Tech. Education, ATBU Bauchi. All rights reserved

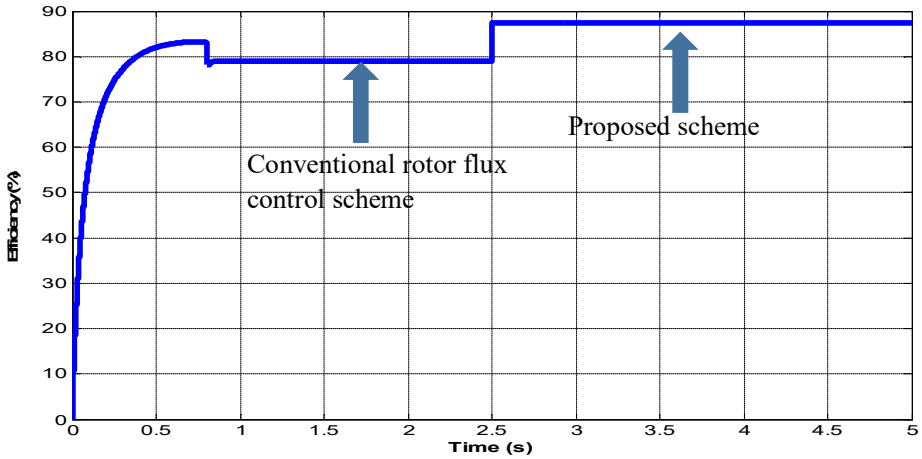

Figure 25: Efficiency of the motor with load torque varying from 3Nm to 2Nm

This implies that the efficiency is maximized for all loads under the scheme. These results follow the same trend as the results provided in Aygun and Aktas (2018). The advantage of the scheme proposed in this work is that the point of maximum efficiency is higher by 5.01%. Table 8 gives a comparison between the results obtained in this work and those obtained in Aygun and Aktas (2018) when the load torque varied from 3Nm to 2Nm.

Table 4.8: Comparison of Optimized DTC and Proposed Method at Variable Load.

Scheme	Total power loss (W)	Efficiency (%)
Proposed method at 3Nm	108.04	87.41
Proposed method at 2Nm	72.03	87.41
Optimized DTC at 3Nm	166.28	82.4
Optimized DTC at 2Nm	110.3	82.4

The results suggest that the point of maximum efficiency is independent of the load torque but the optimum flux at which it occurs depends on the load torque.

The voltages supply to the stator windings of the three-phase induction motor are shown in Figure 26

Corresponding author: Balogun, F. O.
Odunayobalogun2001@yahoo.com
Department of Electrical Engineering, Faculty of Engineering, Ahmadu Bello University, Zaria.
© 2023. Faculty of Tech. Education, ATBU Bauchi. All rights reserved

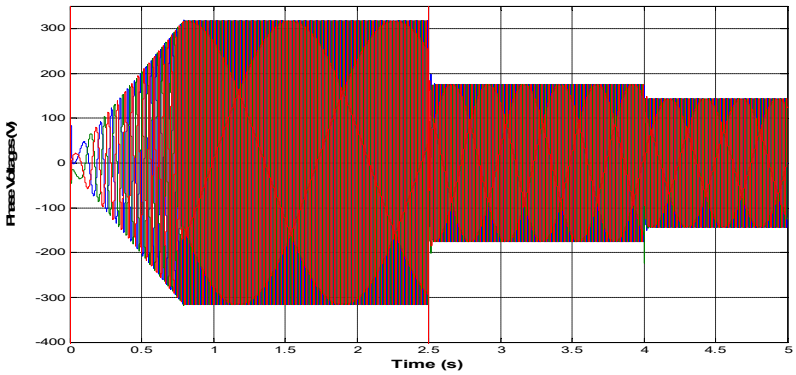

Figure 26: Three phase voltages supplied to the induction motorwith load torque varying from 3Nm to 2Nm

It can be seen that the magnitude of the stator voltages reduces with load on the machine. This is an inherent energy saving measure of the proposed rotor flux optimization control strategy. The reduction in voltage is a direct result of the significant reduction in flux to its optimal levels for each load. The magnitude of the stator voltages rises during motor acceleration. It reaches a value of 311V at steady state while the load torque of 3Nm is applied. The value reduces to 180V after the optimizing control algorithm is activated at 2.5s. The value further reduces to 150V after the load torque changes from 3Nm to 2Nm.

CONCLUSION

This research shows that the proposed flux optimization model significantly improves the conventional rotor flux control drive of the three-phase induction motor. A comparison of the conventional and proposed rotor flux oriented control drive shows that when the reference speed was set to 250rad/s at a load torque of 3Nm, the rotor flux reduced from a rated value of 1Wb to an optimal value of 0.6357Wb thereby leading to a significant reduction of the total power loss from 200W to 108.04W and a consequential increase in efficiency from 78.9% to 87.41%. The performance of the scheme at varying load also shows a change in optimum flux from 0.6357Wb to 0.5188Wb after the load torque was reduced from 3Nm to 2Nm. Although the motor operated at a lower load torque, the flux optimization function of the proposed scheme maintained a maximum efficiency of 87.41%. The proposed scheme showed that while the point of maximum efficiency is independent of the load torque, the optimum flux at which it occurs depends on the load torque. With the proposed drive scheme operating at variable speed mode in which motor speed was ramped down from 250rad/s to 150rad/s at a load torque of 3Nm, power loss is observed to further reduce significantly from 108.04W to 83.645W giving a reduction of 22.6%.

REFERENCE

Aygun, H., & Aktas, M. (2018). A novel DTC method with efficiency improvement of IM for EV applications. *Engineering, Technology &*

Corresponding author: Balogun, F. O.
Odunayobalogun2001@yahoo.com
Department of Electrical Engineering, Faculty of Engineering, Ahmadu Bello University, Zaria.
© 2023. Faculty of Tech. Education, ATBU Bauchi. All rights reserved

Applied Science Research, *8*(5), 3456-3462.

Engel, E., Kovalev, I. V., & Karandeev, D. (2015, September). Energy-saving technology of vector controlled induction motor based on the adaptive neuro-controller. In *IOP Conference Series: Materials Science and Engineering* (Vol. 94, No. 1, p. 012008). IOP Publishing.

Eseosa, O., & Christian, A. (2018). Energy Efficiency Optimization of Three Phase Induction Motor Drives for Industrial Applications. *Int. J. Eng. Appl. Sci*, *5*(8).

Faduyile, O. E. (2009). *Effect of harmonics on the efficiency of a three phase energy efficient and standard motors*. The University of Tennessee at Chattanooga.

Kalhoodashti, H. E., & Shahbazian, M. (2011). Hybrid speed control of induction motor using PI and fuzzy controller. *International Journal of Computer Applications*, *30*(11), 44-50.

Khan, H., Hussain, S., & Bazaz, M. A. (2015, August). Direct torque control of induction motor drive with flux optimization. In *2015 International Conference on Advances in Computing, Communications and Informatics (ICACCI)* (pp. 618-623). IEEE.

Laroui, M., Nour, B., Moungla, H., Cherif, M. A., Afifi, H., & Guizani, M. (2021). Edge and fog computing for IoT: A survey on current research activities & future directions. *Computer Communications*, *180*, 210-231.

Le, P. M., Le, D. D., Nguyen, T. V., & Nguyen, P. H. (2013). Real-time loss minimization control in induction machines based on DSP TMS320LF2812. *Science and Technology Development Journal*, *16*(4), 5-18.

Nam, S. W., & Uddin, M. N. (2006, July). Model-based loss minimization control of an induction motor drive. In *2006 IEEE International Symposium on Industrial Electronics* (Vol. 3, pp. 2367-2372). IEEE.

Rashtchi, V., & Bizhani, H. (2015). Using of particle swarm optimization for loss minimization of vector-controlled induction motors. *Universal Journal of Electrical and Electronic Engineering*, *3*(3), 71-80.

Sruthi, M. P., Nagamani, C., & Ilango, G. S. (2017). An improved algorithm for direct computation of optimal voltage and frequency for induction motors. *Engineering science and technology, an international journal*, *20*(5), 1439-1449.

Yadav, J. G. Optimal energy control of three phase induction motor drives.

Corresponding author: Balogun, F. O.
✉ *Odunayobalogun2001@yahoo.com*
Department of Electrical Engineering, Faculty of Engineering, Ahmadu Bello University, Zaria.
© 2023. Faculty of Tech. Education, ATBU Bauchi. All rights reserved